Chapter 8 Main Tracking Detectors

8.1 Introduction

The principal task of the tracking system is to provide efficient reconstruction of charged-particle tracks and precise measurements of their momenta. It also has to provide measurements of track directions in both x and y projections for the reconstruction of Cherenkov rings in the RICH detectors. Finally, tracking hits are used in the Level-1 and Level-2 triggers.

The main tracking system comprises eleven tracking stations, situated between the Vertex Detector vessel and the calorimeters. These are shown as T1—T11 in Fig. 2.5. The geometry of the detectors and the choice of technologies are motivated by the requirement of low occupancies. The required spatial resolution is then easily satisfied. Most of the detector acceptance is subject to a particle density which is low enough to use drift chambers with small cells. This Outer Tracking System consists of straw-tube-like chambers. The Inner Tracking System covers (in most stations) an area of 60×40 cm^2 around the beam pipe, where a much finer granularity is necessary. For this inner region several alternative technologies are under study.

The tracking system provides precise particle trajectories in the bending plane of the spectrometer using near-vertical wires and strips. Three dimensional track reconstruction is achieved using small stereo angles of $\pm 5°$. The stations situated up- and downstream of the RICH detectors are equipped with additional planes which provide precise measurements in the non-bending projection. These allow precise measurements of the track direction in both projections.

A track reconstruction program [1] has been developed, based on the technique of Kalman filters. For most tracks, the reconstruction is started by following tracks in the upstream direction. A track seed is found in station T10, which defines a search window in the next station, T9. The track is then followed, station by station into the Vertex Detector. In each station, the newly associated hits are used to update the track parameters. Using seeds found in the Vertex Detector, a second pass, in the downstream direction, reconstructs those tracks which leave the acceptance of the spectrometer before they reach station T10 and extrapolates the remaining tracks through T11 and into the muon detectors.

The track reconstruction program is used to design the layout of the tracking system and to optimize its performance. Details are given in Ref. [1]. Stations T10 to T7 are used for track finding. In this region, there is almost no magnetic bending and redundancy is high, since the distance between the stations is small. The momentum measurement of the particles is provided principally using stations T6 to T3. The precision is dominated by multiple scattering, so the number of stations in this region is minimized. This also reduces the number of photon conversions. The distance between two stations is chosen so that less than 10% of the search windows contain a second track.

Chambers in the high magnetic field, close to the centre of the magnet, have a higher occupancy due to curling low-energy tracks. Access for cables and services is also limited in this region. Hence, the number of stations inside the magnet is kept as low as possible.

The stations T2 and T1 do not contribute significantly to the momentum measurement. They are required to link the tracks from the main tracking system to the track segments in the Vertex Detector. These stations are crucial for track following in the downstream direction, where the track segments found in the Vertex Detector are extrapolated through the magnet.

The Monte Carlo simulations of occupancies and the radiation levels presented in this chapter are based on the nominal LHCb luminosity of $\mathcal{L} = 2 \times 10^{32}$ cm^{-2} s^{-1}, which corresponds to an average of approximately one interaction every four bunch crossings. The LHCb experiment has to deal with particle densities which are similar to those experienced at HERA-B. The tracking detectors proposed for LHCb have a layout and employ technologies which are similar to those in HERA-B. The consequences related to short-term operation with higher luminosities (a maximum of $\mathcal{L} = 5 \times 10^{32}$ cm^{-2} s^{-1} is considered) differ for the

Table 8.1: Dimensions of the active area in the Inner Tracking System.

Station	z cm	$\Theta_{\min}$ mrad	$x, y_{\min}$ cm	$x_{\max}$ cm	$y_{\max}$ cm
T1	100	50	5.0	35	35
T2	229	16	3.6	30	30
T3	321	14	4.5	30	20
T4	416	12	5.5	30	20
T5	556	12	6.9	30	20
T6	691	12	8.2	30	20
T7	781	12	9.1	30	20
T8	831	12	9.6	30	20
T9	881	11	10.1	30	20
T10	928	11	10.5	30	30
T11	1174	11	13.0	30	30

different detector technologies and are referred to in the following sections.

8.2 Inner tracking detectors

The Inner Tracking system covers the region around the beam pipe, where the particle flux is too high for conventional drift chambers. The positions and dimensions of the stations are summarized in Table 8.1. The outer boundaries are defined by the occupancy requirement in the outer tracker cells. Since the particle flux at a given distance from the beam varies only slowly with z, this boundary ($60{\times}40$ cm^2) is the same in most stations. The stations immediately up- and downstream of the RICH counters include horizontal wires (or strips). To reduce the occupancy in the horizontal wires of the outer tracker, the inner tracker has dimensions $60{\times}60$ cm^2 in these stations. The inner boundaries are defined by the conical beam-pipe.

Station T1 is special. The outer tracker would only cover a small region, which makes it more economical to construct T1 entirely using the inner detector technology. This station is situated close to the last disc of the Vertex Detector and does not have to cover the region close to the beam-pipe.

Several detector technologies meet the requirements of the inner tracker. Three options are decribed here. The MSGC/GEM detector has been chosen as the basis for cost estimates, although further R&D is required. The well-proven fall-back solution, silicon strip detectors, is estimated to be significantly more expensive. To reduce costs even further, a new type type of detector, the MCSC, is currently being investigated. The process and time schedule for making the technology choice is described at the end of the section.

8.2.1 MSGC/GEM detectors

The proposed microstrip gas chamber (MSGC) inner detector is based on the development and test of similar detectors for HERA-B. Particle rates and radiation doses expected at LHCb are about the same as those in HERA-B, which therefore provides an ideal test of the technology. There are some differences however. The bunch-crossing frequency at LHC is four times higher than at HERA. This requires a faster shaping of the signals, and different detector dimensions to limit the maximum drift times. In addition, the maximum Level-0 trigger rate is ten times higher at LHCb with corresponding requirements for the readout system. The detector for LHCb, described below, is based on presently available and tested technology with only minor ('safe') changes compared to the HERA-B detectors. Directions for further improvements are discussed below.

Severe aging and operation problems with MSGC detectors have been reported. The introduction of conductive 'diamond'-coating of the substrates, in combination with the use of appropriate materials and gases, has solved the aging problems and has led to detectors with good spatial homogeneity, good high-rate behaviour and a remarkable robustness of operation even in the presence of defects in the electrode or surface structure. A major problem was, however, the observation that MSGC's show gas discharges when operated at 'useful' gains of $\sim$ 3000 in intense hadron beams. These discharges gradually destroy the electrode structures. The problem has been solved by the introduction of an additional amplification stage using a gaseous electron amplification (GEM) foil [2] on top of the MSGC. With a typical gain of 20 at the GEM, the gas amplification of the MSGC can be reduced below 200. The HERA-B inner tracker has shown that MSGC/GEM detectors, operated with Ar:DME 50:50, have excellent high-rate properties, show no gas discharges in intense hadron beams, and no aging up to integrated doses of at least 8 mC/cm strip length (equivalent to more than three years of LHCb operation at nominal luminosity). Similar results have been obtained by a CERN group using an Ar:CO_2 mixture [3]. Further tests at higher integrated doses are underway. It has also been shown that the detectors can be operated in a magnetic field (0.85 T) without loss of

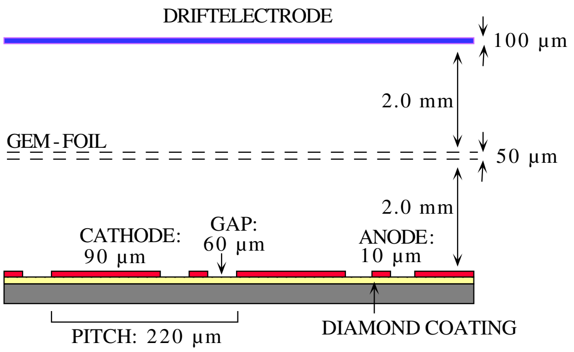

Figure 8.1: Schematic cross section through a MSGC/GEM detector (not to scale).

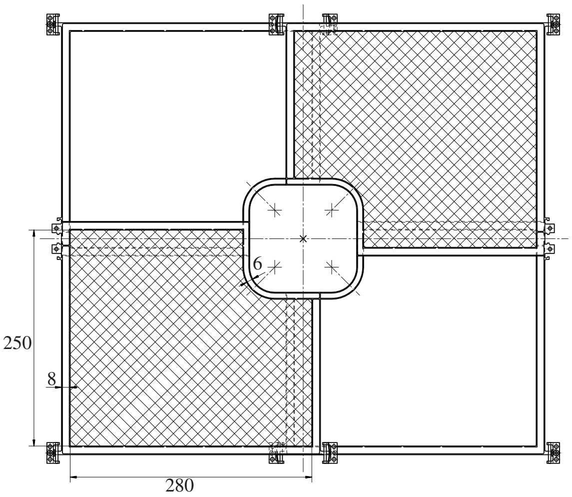

Figure 8.2: Front view of one inner tracking layer consisting of four overlapping detectors. Dimensions are mm.

efficiency and resolution. The LHCb dipole magnet produces 1.1 T, so these results require confirmation at the higher field.

Detector configuration

A cross section through a typical detector is shown in Fig. 8.1. It has dimensions of $\sim 28 \times 25$ cm^2 with a corner removed to accommodate the beam pipe. One layer is made of four overlapping detectors, having the same strip orientation, covering the sensitive region around the beam pipe. A view of the detector geometry for one layer is shown in Fig. 8.2.

The MSGC electrode structure for one chamber is manufactured on a single AF45 glass substrate with a conductive 'diamond' coating ($\sim 10^{15}\Omega$/square). The electrodes consist of gold (500 nm thick) with a pitch of 220 μm, an anode width of 10 μm separated from the cathode by a gap of 60 μm. The technology required to produce MSGC plates of this dimension has been established by the HERA-B production process[1]. The GEM foil is kapton, 50 μm thick, and coated with $2 \times 5\mu$m of copper. It has 60 μm holes, staggered with a pitch of 140 μm. These GEM foils are produced in the CERN workshop with good yield and quality. They allow safe operation at high rates up to gains of about 50 (operation at a gain of about 25 is preferred). GEM's coated with a diamond layer show good stability and a much improved spatial homogeneity of the gain. The chamber construction is based on two hollow G10 frames, 8 mm wide and 2.0 mm high, which define the gas volume above and below the GEM foil. This frame is also used for the gas distribution in the detector. The chamber is closed by the drift electrode consisting of an aluminium-coated kapton foil (100 μm thick). The detector components are glued together using UHV epoxy glue. This chamber construction is presently used for HERA-B except that the gap heights are 3.0 mm for HERA-B instead of 2.0 mm.

The effective detector thickness in the sensitive area, including support structures, is 0.55% X_0. The frame, which is 8 mm wide and covers 11% of the area, has a thickness of 1.0% X_0 . The sensitive area starts at least 16 mm from the beam-pipe. The MSGC inner tracking system has a total of ten stations (if T1 is assumed to use silicon detectors), each with four detector layers having vertical and near-vertical strip orientations ($90°, 95°, 85°, 90°$). Including the horizontal-strip layers in T2, T10 and T11, this results in a total of 43 layers and 172 MSGC/GEM detectors each with 1280 strips. The total sensitive area covered is 13.5 m^2, equipped with 221000 readout channels. This is similar to HERA-B where an area of 10.1 m^2 is read out by 140000 strips.

Operation characteristics

The gas gain achieved in an Ar:DME 50:50 mixture is shown as a function of cathode voltage in Fig. 8.3 for different GEM voltages. The dramatic reduction of cathode voltage which can be achieved for the same gas gain using the GEM technology is clearly visible.

[1] Substrates of the necessary size (up to 30×30 cm^2) are produced commercially. Diamond coating is presently produced by the Fraunhoferististut for Surface engineering and thin films, Braunschweig, Germany. Electrode structures are produced by IMT, Greifensee, Switzerland.

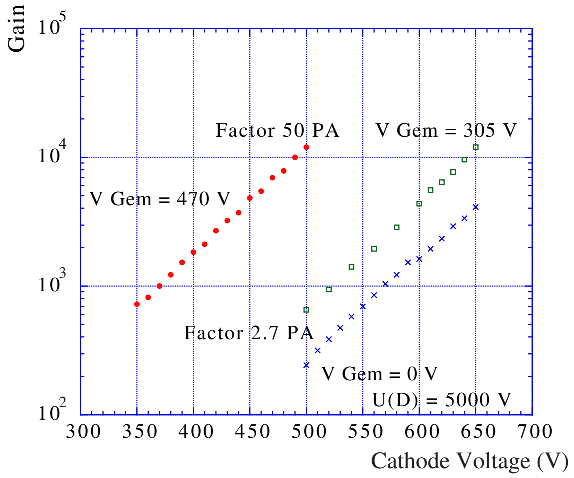

Figure 8.3: Gas gain for a MSGC/GEM detector with Ar-DME 50:50 mixture.

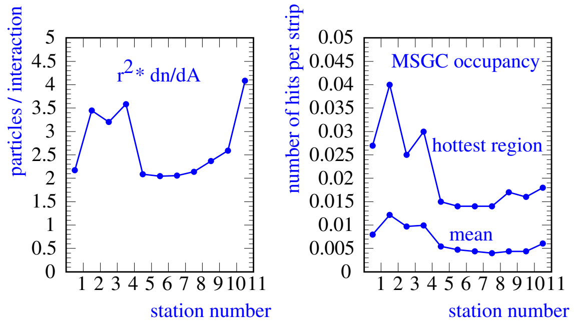

Figure 8.4: Particle density per cm^2 for one interaction multiplied by r^2 [cm^2] in each station (left). Maximum and mean occupancy in each station at nominal luminosity (right).

This gas mixture provides high primary ionization, reliable operation and good aging properties. It has been extensively tested and will be used for HERA-B. The chamber operates with a drift field of about 7.5 kV/cm resulting in a drift velocity of 52μm/ns and a maximum drift time $\leq$ 40 ns. For operation in the magnet (1.1 T) the Lorentz angle at 7.5 kV/cm is about 9°, the expected strip multiplicity is 1.55 and the precision $\leq$ 65 μm.

The mean primary ionization of 15 e^-, a gas gain of 4000 and an effective integration time of 25 ns (50 ns pulse duration) lead to a mean detected signal of 22000 e^-/MIP. This is adequate for a good signal-to-noise ratio and an efficiency > 95% (assuming noise of $\leq$ 1400 e^-). The high gain which can be guaranteed by the MSGC/GEM technology is crucial. They show however a rate dependence of the gain due to charge-up and polarization effects which also lead to local inhomogeneities in the gas gain. Recently GEM's have been tested for HERA-B, where the GEM's are coated with a diamond layer. These show very good stability of gain and the homogeneity of the gain over the detector area is about 10% for diamond-coated GEM's, compared with 30% for the uncoated GEM's.

The expected maximum and average occupancies for the proposed LHCb detector layout are shown in Fig. 8.4. The occupancy never exceeds 4%. Correspondingly the maximum integrated charge per cm of strip-length is $\leq$ 2.5 mC/cm per year at nominal luminosity. It is assumed that strips which fire in one bunch crossing are disregarded in the next bunch crossing. Pile-up will not, therefore, increase the occupancy but will decrease the efficiency. These operating conditions provide adequate performance at the nominal LHCb luminosity. Faster gases with high primary ionisation are clearly desirable for high luminosity running and will form part of the LHCb-specific R&D programme.

Read-out electronics

The readout of the inner tracker has to provide the following:

- Fast shaping of signals to cope with the 25 ns bunch-crossing rate;
- Deadtimeless storage (or readout) of the strip information at the maximum Level-0 trigger rate of 1 MHz;
- Fast trigger signals for the Level-1 tracking triggers, for all events accepted by Level-0.

None of the readout chips developed for HERA-B or LHC is able to satisfy all requirements. The readout chip development for MSGC/GEM detectors could however benefit from the experience and partly from the design and layout of the HELIX128 chip developed at Heidelberg for the HERA-B strip detectors. The following developments are necessary:

- A new input stage with faster shaping;
- Radiation hard technology. The transfer to DMILL is already planned by HERA-B.
- A new data storage and readout scheme. Analogue data is stored in the Level-0 pipeline (see Fig. 8.5). Following the Level-0 trigger, two possible readout schemes are

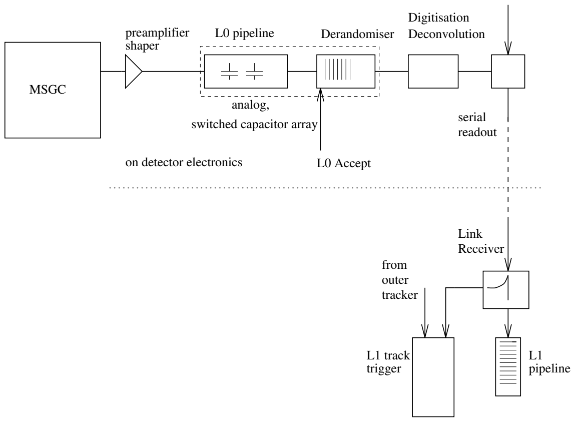

Figure 8.5: Schematic of the MSGC readout system.

considered, both requiring a substantial R&D effort.

  - Multiplexing of 32 channels and analogue readout at 40 MHz, followed by analogue deconvolution and digitization in the link receiver.
  - Digitization and read out with 3 bits per bunch crossing, using a GHz link for every 256 channels.

In both schemes the Level-1 trigger signals are derived from the Level-0 data buffers.

Supports and infrastructure

Detailed solutions for the chamber mechanics, cabling, gas and HV supplies have been worked out for HERA-B and can be used with minor modifications for LHCb. Each station is rigidly fixed and aligned to the outer tracking detectors.

Future R&D

The detector development and testing of the baseline MSGC/GEM solution will be done within the HERA-B project. In 1998 a fully equipped station will be operated in HERA-B. Mass production of detectors also starts early in 1998. This important field test will allow a realistic evaluation of the detector technology and performance by the end of this year.

LHCb-specific developments towards improved detector technology include:

- Optimization of the GEM technology.
- Investigation of faster gas mixtures with high primary ionization.
- Reduction of material, for example, through the development of 2-dimensional readout.
- Testing of advanced GEM technologies which might avoid the use of MSGC plates altogether.

8.2.2 Silicon Micro Strips

Silicon-strip detectors are well-proven and considered as a fall-back solution. They offer the following advantages:

- The occupancy is less than 2.5% per channel with a readout pitch of 250 μm.
- The resolution (< 100 μm) is more than sufficient.
- Silicon detectors can sustain high doses of radiation.
- No gases are involved.

The main argument against the choice of Si-strip detectors is the cost. However, if the number of readout channels is reduced, by using a large strip size or by combining strips, the cost can be comparable to that of other technologies.

Detector layout

Single-sided Si-detectors, similar to those used in the Vertex Detector are proposed. The advantages over double-sided detectors are:

- Simplicity of design, with readout only on one side of the detector.
- Single-sided p-on-n detectors remain operational after sustaining significant radiation doses.[4]

The disadvantage is that the detector will be thicker overall.

Four layers per station are proposed: Y, U, V, and Y, with strip orientation 90°, 85°, 95°, 90°. All layers are identical and orientation is provided by rotating the whole layer. Overlap is provided by shifting layers slightly with respect to each other. The stations nearest the RICH detectors need a fifth layer in the X direction (0°).

Each layer is formed from ladders of daisy-chained Si-detector modules. A layer of 60×40 cm^2 is built up of 12 short modules, (6×7.5 cm^2 of silicon) and 22 long ladders of two modules each, shown in Fig. 8.6. The hole for the beam pipe varies in size according to the location of the station. The

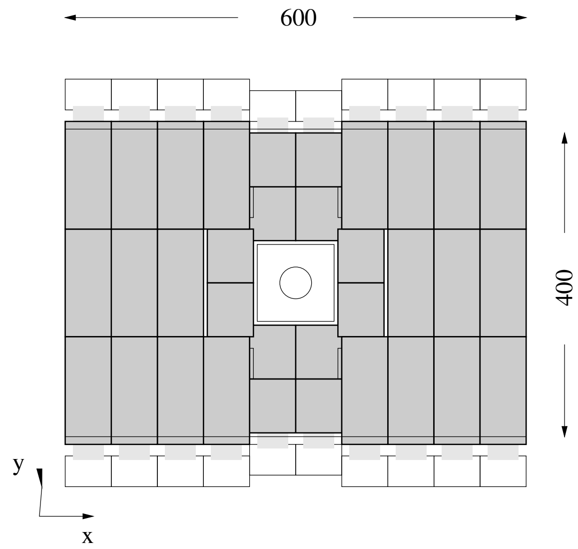

Figure 8.6: Layout of Si-detector ladders in a layer. Dimensions are mm.

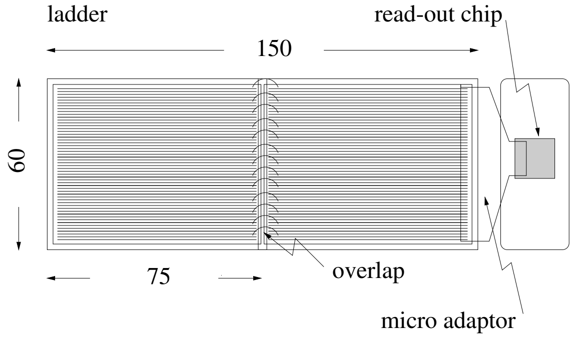

Figure 8.7: One ladder mounted on a carbon-fibre support.

smallest size is $x_{\min} = y_{\min} = 3.6$ cm. The layout of the ladders will differ from station to station, requiring a specific support structure for each station. The ladders themselves, however, are identical for all stations. They are mounted as "roof tiles", in order to avoid dead space.

Detector design

The proposed Si-strip detectors are 300 μm thick, with a strip pitch of 125 μm. Single-sided readout of every second strip is foreseen, so that the readout pitch is 250 μm. The Si-modules will be glued onto carbon fibre supports and the strips bonded together in ladders as shown in Fig. 8.7. The readout chips are mounted on hybrids and glued onto the carbon-fibre support. They are bonded to the strips via pitch adaptors.

A stainless steel pipe with 2 mm diameter and 40 μm wall thickness is glued to the back of the assembly. Liquid at a temperature close to 0°C flows through this pipe and removes heat from the readout chips. It also helps to protect the Si-detectors from radiation damage. LHCb participates in a common evaluation of cooling techniques for LHC silicon detectors.

The amount of material a particle sees when it traverses a ladder corresponds to 0.51% X_0. Most of this (0.28% X_0) is due to the silicon. At the location of the cooling pipe, the material amounts to 1% X_0. To avoid "hot spots", the four layers which make up one station have their cooling pipes staggered. The overall material budget per station amounts to 2% X_0 on average.

Readout electronics

The readout electronics system used for the Vertex Detector will satisfy the requirements for the silicon detectors proposed here. At a readout pitch of 250 μm, there will be 240 channels/module (2 readout chips), 34 modules/layer (= 8160 channels/layer) resulting in $\simeq$ 32640 channels/station. Equipping all inner tracking stations with Si-detectors implies a total of about 350000 channels.

Signal to Noise ratio

The electronics noise in a silicon detector system depends on the properties of the preamplifier/shaper and of the silicon detector itself. Series noise is mainly determined by the capacity of the strip. The maximum strip length in the proposed detectors is 14 cm, corresponding to a capacity of 26 pF.

The noise is estimated for an amplifier-comparator chip with a rise time of 30 ns as used in Ref. [5]. The noise, expressed in electrons (ENC), as a function of the input capacitance parametrised [6] as

$$\mathrm{ENC} = (730 + 31.5/\mathrm{pF} \times C), \qquad (8.1)$$

yields ENC $\simeq$ 1500 electrons.

The MIP signal in a 300 μm thick silicon detector is about 25000 electrons, which implies a signal-to-noise ratio of 16 : 1. However, approximately 30% of the signal is lost to the capacitively coupled non-readout strip, which reduces the ratio to about 11:1. This is sufficient for good tracking.

Radiation hardness

The minimum inner radius of the Si-strip detectors in the Inner Tracker is 3.6 cm. At this radius, particle fluxes are about ten times lower than at the inner edge of the Vertex Detector, and decrease rapidly with distance from the beam. Since the high radiation dose is localised, the ladders could be recycled within one layer, i.e. by exchanging modules closest to the beam with those further away. We are confident that an inner tracking detector based on silicon microstrips can work. An R&D programme, together with the Vertex Detector group, will be carried out to determine an optimal solution taking into account physics performance, technology, cost, and the possible replacement and/or recycling of parts of the inner tracker after a few years of operation.

Future R&D

A prototype ladder will be produced, in order to test the mechanical aspects, the cooling aspects and the radiation hardness. Ideally, the prototype should be tested in an LHCb-like environment, e.g. near the HERA-B beam pipe. This development programme will be coordinated with that required for the silicon Vertex Detector modules.

8.2.3 Micro Cathode Strip Chambers

Micro Cathode Strip Chambers (MCSC's) measure analogue signals induced on narrow cathode strips, orthogonal to and separated by 0.6 mm from the anode wires. The geometry of the proposed device is shown in Fig. 8.8 and described in detail in Ref. [7]. The inner tracking stations are divided into several such MCSC modules.

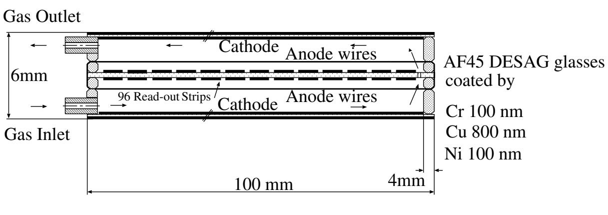

Figure 8.8: Schematic of the MCSC chamber.

Precise coordinate measurement in a high particle flux requires a fast, low-noise front-end preamplifier/shaper. Prototype detectors have been tested in beams at CERN and with X-ray sources. The results [7] demonstrate that MCSC's can meet the basic requirements for the inner tracker. A detailed simulation of the MCSC chamber, which includes the gas processes, noise and electronics response has shown good agreement [8] with the results obtained in the tests. An output signal with a peaking time of 20 ns and a full width of less than 50 ns was observed. The ADC must measure the collected charge with 8-bit precision. The design of the readout system [9] requires R&D effort to meet the requirements that are specific to LHCb.

An attractive feature of the MCSC option for the LHCb inner tracking system is that it could cover the area with less than half the number of readout channels, compared to the other options, however at the cost of higher occupancy.

8.2.4 Inner Tracker technology decision

All three inner tracking options have been implemented into the Monte Carlo simulation, which includes the appropriate material thickness, intrinsic spatial precision and occupancies. The results confirm that the measurement of the relevant physics parameters does not depend significantly on the choice of the technology.

The most important criteria for the choice will be reliability and cost. For each of the options, a programme of investigations will be defined with milestones. This programme will include studies of detector technologies, their implementation in the experiment, and also the readout electronics; in particular the development of chips compatible with LHCb requirements.

The inner tracker is a relatively small system which can be built and installed in less than two years. However, the time required to develop readout chips is much longer. The time scale for the inner tracker decision will need to be coordinated with the overall management of the front-end electronics.

In the cost estimate of the detector, silicon microstrip detectors have therefore been assumed for station T1, and MSGC's for the remainder. The particle flux is particularly high in the innermost part of the tracker in the stations situated in the magnet (see Fig. 8.4). Inner tracker stations of hybrid technology, i.e. MSGC's or MCSC's with a 10×10 cm^2 silicon insert around the beam pipe are also considered for this region.

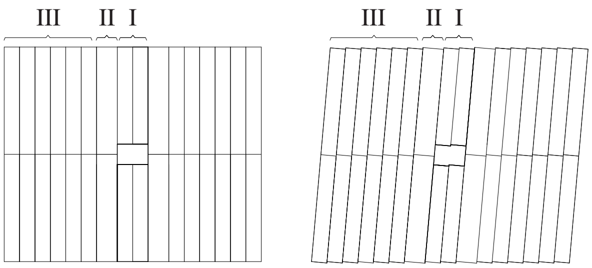

(a) Vertical Wires (b) Stereo Wires

Figure 8.9: Modularity of detector planes. Module types I and II have 5 mm cells. Type III has 8 mm wide cells and is used in stations T7 – T11.

8.3 Outer tracking detector

8.3.1 Detector geometry

The outer detector consists of drift cells with straw-tube geometry. The configuration of each tracking station is summarized in Table 8.2. Since the emphasis is on tracking precision in the (x, z) bending plane, electron drift in most of the detector planes is in or near the x-direction. Stations T2 – T10 contain two planes with vertical sense wires, and two planes where the wire directions are tilted by $+5°$ and $-5°$ from the vertical (U and V in Table 8.2). In stations adjacent to a RICH detector, two additional planes with horizontal sense wires provide track directions with similar precision in the x- and y-projections. In station T11, just downstream of RICH 2, the $\pm 5°$ stereo views have been omitted. They are not needed here because approximate space points provided by the nearby muon pad-chamber resolves stereo ambiguities.

Each plane listed in the table contains two staggered layers of drift cells. A "standard" station (T3 – T9) contains 4 x 2 = 8 cell layers in total. Figure 8.9 shows the schematic layout of a plane with (a) vertical or (b) stereo wires. A plane is assembled from modules with widths of 48 (type I), 64 (type II) or 32 (type III) cells per layer. Types I and II have 5 mm diameter cells, type III has 8 mm cells. Although a module of type II or III spans the full vertical extension of a station, the sense wires are split at $y = 0$. Thus, front-end electronics are mounted along the top and bottom edges of a station. Similarly, planes with horizontal sense wires carry front-end boards at the left and right edges. At a large distance from the beampipe, type III modules are split into two halves, not due to occupancy considerations but to reduce signal propagation time along the sense wire.

To keep the occupancy per cell below 10%, modules of type I are active only down to $|y| = 19$ cm, and modules of type II down to $|x| = 29$ cm. This leaves a rectangular hole around the beampipe, which is covered by the Inner Tracker. Simulation studies [10] show that the highest cell occupancy per interaction is 10%, occurring in the innermost cells of stations T2 and T11. One module of type II is necessary on either side of the beam pipe before switching to a larger cell size (type III, starting at $|x| = 68$ cm).

In addition to occupancy, signal latency is a major concern. The delay in signal arrival time at the preamplifier is the sum of drift time and propagation delay along the sense wire. The maximum propagation delay varies from about 4 ns in station T2 to as much as 17 ns in the horizontal wires of T11. For fast drift, a gas mixture containing CF_4 is needed. However, the possibility that detectors in or near the magnet, in stations T2 – T6, will be operated with a different mixture than stations T7 – T11 is being investigated. The drift times and trajectories have been studied with a detailed simulation program [11] which faithfully reproduces measurements [12] with honeycomb chambers. Tests of fast drift gases are in progress. We will also benefit from experience at HERA-B where a CF_4-based mixture is used. Outside the magnetic field, the drift time in a 5 mm cell can be kept below 20 ns using CF_4:CH_4, Ar:CF_4:CO_2 or Ar:CF_4:CH_4 mixtures. In a field of 1.1 T, the maximum drift time in such a cell can be kept below 30 ns. However, the effective drift velocity $v_d \times \cos \alpha_L$, where α_L is the Lorentz angle, drops quite sharply at larger distances from the sense wire (the best result obtained with a 10 mm diameter cell is a maximum drift time of 85 ns). Therefore, stations T2 – T6 will have 5 mm diameter cells, even though occupancies would allow a larger cell size. In stations T7 – T11 the choice of cell size for the type III modules is 8 mm. With the HERA-B drift gas this will result in collection of all drift signals within 50 ns (two bunch-crossing intervals). The choice of a CF_4-based drift gas entails some loss in precision due to electron attachment. The single-cell resolution is expected to be in the range 150—200 μm, which is adequate for momentum precision (see Section 8.5).

The fact that signal latency extends to two bunch-crossing intervals instead of one, has important consequences. The Level-1 track trigger must always consider two 25 ns time slices of pipelined data and track reconstruction will include signal overlap from interactions in consecutive beam crossings. At nominal LHCb luminosity

Table 8.2: Outer dimensions, arrangement of detection planes and numbers of readout channels for the Outer Tracking detector stations

station	z_{mean} (cm)	active area $x_{\max}$ (cm)	$y_{\max}$ (cm)	planes (wire orient.)	channels 5 mm cells	8 mm cells
2	217	75	75	X X Y U V Y	6.0 k	
3	330	191	154	Y U V Y	10.2 k	
4	425	191	154	Y U V Y	10.2 k	
5	565	191	154	Y U V Y	10.2 k	
6	700	217	179	Y U V Y	11.6 k	
7	790	244	202	Y U V Y	3.6 k	6.3 k
8	840	260	214	Y U V Y	3.6 k	6.8 k
9	890	275	227	Y U V Y	3.6 k	7.4 k
10	940	291	240	Y U V Y X X	5.4 k	11.0 k
11	1165	360	297	Y Y X X	3.6 k	9.3 k
					68.0 k	40.8 k

there is about a 50 % chance that an accepted event contains hits from an interaction in either the preceding or the following bunch crossing.

The overall layout of the LHCb Outer Tracker is quite similar to that of the HERA-B experiment. The HERA-B Outer Tracker consists of 13 stations, at distances from about 2 m to 13 m from the target region. The largest station has a sensitive surface of 6m×4.5m. Each station consists of the same three stereo views (0,±5°) as are used in LHCb, but there are no horizontal wires. The inner hole around the beampipe is 20cm×20cm, and cell occupancies in HERA-B can be as high as 20%. However, at the 96 ns bunch interval of the HERA proton beam, overlap of signals from consecutive bunch crossings can be avoided.

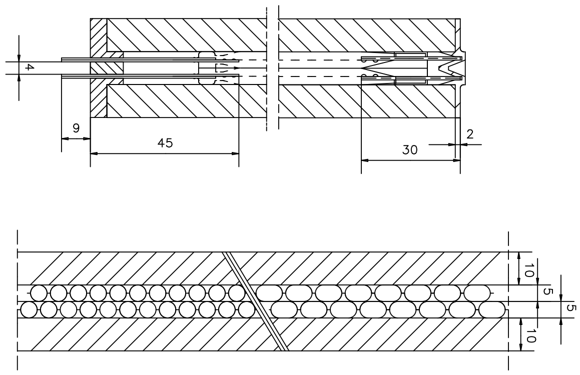

Figure 8.10: Details of the end-pieces of module type I (top). Cross section of the border region between 5 mm and 8 mm cells (bottom): all dimensions are (mm)

8.3.2 Detector design

Detector modules will be constructed using a similar procedure as for HERA-B. A cell layer is produced from two preformed conductive foils. Instead of the true honeycomb structure employed by HERA-B, the LHCb design uses two staggered cell layers in a module. Vacuum forming of the cathode foils is currently being tested. However, should this prove unsatisfactory, the folding machine used for the HERA-B production is still available. Figure 8.10 shows cross sections of modules with 5 and 8 mm wide cells. A module provides its own rigidity, defines its own gas volume and has its own high voltage and front-end boards. The 5 mm cells have a circular cross section with two slightly flattened sides, the 8 mm wide cells are flattened to the same depth as the 5 mm cells. The pitches are 5 + 1 = 6 mm and 8 + 1 = 9 mm. A flat conductive foil separates the two cell layers. This layout offers the following advantages with respect to a true honeycomb structure:

- It is easier and cheaper to build;
- There is no need for a hexagonal cell shape, which suffers from low drift fields near the sharp corners;
- In the proposed layout the fraction of active area per cell layer is 5/6 (5 mm cells) or 8/9

(8 mm cells) while it is only 2/3 in a full honeycomb structure.

The choice of foil material is still open. Prototypes have used the same carbon-doped polycarbonate (trademark Pokalon) from which the HERA-B chambers have been built. The HERA-B chambers successfully withstood extensive aging tests with X-ray and beta sources, but stability problems have been observed in hadron beams. Independent of whether the problem is associated to the foil material, the same product will not be used for the LHCb outer detector, since it is no longer commercially available. Materials with volume conductivity (like Pokalon) or the use of a conductive surface layer are both under consideration for the cathode foil.

It follows from the cell geometry that the average hit multiplicity per track in a module is 5/3 (5 mm cells) or 16/9 (8 mm cells). For all realistic track angles, a particle passing through an insensitive region of one layer will hit a cell in the other layer in a region of almost 100 % efficiency. Efficiency near the cell edges depends not only on the cell shape, but also on the final choice of drift gas mixture (e.g. electron attachment to CF_4). Test results from prototype cells indicate that edge inefficiencies will be negligible compared to the geometrical loss factor, which is included in the LHCb detector simulation.

Module rigidity is provided by 10 mm-thick foam layers clad with 25 μm aluminium facings. Extensions of the inner facing are wrapped around the sides of the cell layers, thus providing the gas envelope. At 1 m intervals the sense wires are supported by isolating strips. The two sense wires of a cell, each covering half of its length, are terminated on a support strip placed halfway along the length of the module.

The geometrical thickness of a module is 30 mm (10 mm for the two cell layers and 10 mm foam on either side). This represents 0.4 $\%X_0$, assuming the same foil thickness (75 μm) as in prototype modules. There is no further material in the acceptance region, so a standard station of four detector planes represents 1.6 % of a radiation length. Consecutive planes will be mounted (almost) flush against each other, giving a station thickness in the acceptance region of slightly more than 120 mm (180 mm for stations T2 and T10). Outside the acceptance, the total extension in z for the mounting frame, front-end boards, gas distribution and cable paths is 180 mm (240 mm). The joint between adjacent modules in the same plane is 2 mm wide and has a thickness of $5\%X_0$. The terminating structure of modules of type I extends 30 mm into the acceptance of the inner detector (see Fig. 8.10). Over 25 mm, it represents $1.5\%X_0$ per module, and about $8\%X_0$ over the remaining 5 mm closest to the beam pipe.

Stations will be mounted around the beam pipe by sliding left and right halves inwards, on a frame structure. The frame of the outer detector also serves as support for the inner detector, which is supported in front of the outer detector assembly on hollow carbon fibre rods.

8.3.3 Front-End electronics

The number of readout channels required for the Outer Tracking system is given in Table 8.2. It is intended to use the 8-channel ASD-BLR [13] preamplifier/discriminator chip developed by the ATLAS community. It provides ion-tail cancellation tailored to CF_4-based drift gas mixtures, which tend to have very low ion mobility.

Given that the occupancy per interaction will be of order 5 - 10 % in an appreciable fraction of the outer detector channels, the TDC system will be driven by the bunch-crossing clock (rather than being data driven) and will have a Level-0 pipeline for each individual channel. Time measurement within the 25 ns bunch-crossing interval with 5 or 6-bit precision will be sufficient. An 8-channel TDC chip, currently under development at the University of Freiburg, could be adapted. Because of the 50 ns drift window, pipelined cells (following a Level-0 accept) must be fed pairwise to the Level-1 buffer and the track trigger electronics,

In stations inside the magnet coil (T3 – T5) only the preamplifiers will be mounted directly on the detector modules. In the other stations the front-end boards carry the TDC and pipeline chips.

8.3.4 R & D schedule

The design of the mechanics will be frozen by mid 1999; the detailed layout of the front-end electronics about one year later. The most important parameters — choice of drift gas, material and shaping method of the cathode foils — will be fixed before mid '99. A beam test of a telescope of two stations, one placed inside a 1 Tesla field and the other outside the field, is planned in 1998. The test stations will have smaller lateral extensions, but otherwise the geometry will be the same as presently foreseen for the final layout. In addition, a full scale model of a station will be built to test the design of the mounting structure, to verify the assembly procedure and to check the layout of front-end boards, cables, gas lines, etc. Aging tests will be coordinated with the HERA-B outer tracker group. With a gas amplification of a few times 10^4 the accumulated charge in the hottest regions of the outer detector remains below 1 C/cm per year.

8.4 Alignment

It appears very difficult to assemble and to maintain the tracking stations, comprising the inner detectors and the large outer modules, with a precision below 100 μm. Instead, accurate displacement monitoring by means of an optical alignment system is foreseen. Two such systems are used in the ATLAS [14] muon spectrometer. Both systems are fully adequate for the alignment of the LHCb tracker and reach precisions below the 10 μm level. One is developed by MPI and uses an infrared laser and semi-transparent amorphous silicon-strip sensors. The second system, RASNIK, consists of LED's with masks, lenses and CCD's. One device aligns three points with high precision in all three dimensions. More points can be aligned step-wise using several devices. The MPI system can align up to twelve points at a time, and is therefore the baseline option (as in HERA-B) for the alignment of the LHCb inner and outer tracking detectors.

8.5 Performance

The tracking system is designed to provide robust track-finding and track-following. This is obtained with redundant measurements in a relatively large number of layers and stations. The spatial precision is more than adequate and the momentum resolution is limited by multiple scattering. The relative precision, $\delta p/p = 0.3\%$, is approximately constant for tracks of momenta from 5 GeV to 200 GeV [1]. This propagates through to the precision in reconstruction of effective masses. Details are quantified (in Chapter 15) for each of the decay modes used in the physics analysis; examples are B$\rightarrow \pi\pi$ for which the r.m.s precision in mass is 15.2 MeV/c^2 and $\mathrm{D_s} \rightarrow$KKπ (where the $\mathrm{D_s}$ is a $\mathrm{B_s}$ decay product), with a precision of 4.2 MeV/c^2. The contribution of the momentum measurement to the mass precision is comparable with that due to the error in the track angles as measured in the vertex detector. More details on the performance of the tracking system (including the Vertex Detector) are presented in Ref. [1].

References

[1] R.v.d.Eijk , G.Gracia-Abril, M.Merk, O.Steinkamp and W.Ruckstuhl, "Track Reconstruction for LHCb", LHCB/98-045.

[2] F. Sauli, Nucl. Instr. and Meth. A 386 (1996) 531-534.

[3] F.Sauli, private communication.

[4] E.Koffeman, private communication, (L. Andricek et al., in preparation, 1997)

[5] E. Barberis et al., Nucl. Phys. **B** (Proc. suppl.) 32 (1993) 513; E. Barberis et al., IEEE Trans. Nucl. Sci. NS-40 (1993) 740.

[6] E. Barberis et al., Nucl. Instr. and Meth. in Phys. Res. **A** 342 (1994) 90-95.

[7] B.Bochin, et al, "Beam tests of the MCSC prototypes for the LHCb inner tracker", LHCB/98-008; O.Fedin, et al, "Study of MCSC with 36 KeV monochromatic X-rays", LHCB/98-010.

[8] G.Velichko, "MCSC performance simulation", LHCB/98-016.

[9] A.Kashchuk, et al, "Study of fast readout electronics and charge interpolation for MCSC's", LHCB/98-011.

[10] M.Merk, "Digitizations and Occupancies for the LHCb tracking detectors", LHCB/98-044.

[11] R.Veenhof, GARFIELD, "A Drift Chamber Simulation Program", Version 5.05, CERN. S.Biagi, MAGBOLTZ, "A Gas Transport calculation Program", CERN.

[12] RD5 collaboration, A.Bohrer et al, CERN-DRDC-91-53 (1992), CERN-DRDC-92-34 (1992).

[13] M.Newcomer and A.Romaniouk, ATLAS Note INDET-122 (1996); B.Bevensee et al., ATLAS note INDET-80 (1996).

[14] ATLAS Muon Spectrometer, Technical Design Report, CERN/LHCC/97-22.